LASER-ASSISTED SHUNT REMOVAL ON HIGH-EFFICIENCY SILICON SOLAR CELLS

Ngwe Zin[1^], Andrew Blakers[1], Evan Franklin[1], Teng Kho[1], Kean Chern[1], Keith McIntosh[2], Johnson Wong[3], Thomas Mueller[3], Armin G. Aberle[3], Yang Yang[4], Xueling Zhang[4], Zhiqiang Feng[4], and Qiang Huang[4]

[^] Corresponding author: Ngwe Zin, The Australian National University, School of Engineering, North Road, Acton, ACT 0200, Australia. Ph: +61 2 6125 7450, Fax: +61 2 6125 8873, email: soe.zin@anu.ed.au

[1] Australian National University, Australia
[2] PV Lighthouse, Australia
[3] Solar Energy Research Institute of Singapore, National University of Singapore, Singapore
[4] State Key Lab of PV Science and Technology, Trina Solar Limited, China

ABSTRACT

Development of all-back-contact (ABC) silicon solar cells at the Australian National University (ANU), as part of a collaboration between Trina Solar and the Solar Energy Research Institute of Singapore (SERIS), is progressing, and 22.6% efficient ABC cells, based on the aperture-area of 13 cm^2 that excludes busbars, were recently fabricated at ANU. When measured using the 16 cm^2 aperture-area that includes busbars, the cells are 21.7% efficient. In this paper, we demonstrate the technique of removing shunts, associated in the development of ABC cells, by laser-assisted means. The laser that we use for the shunt removal is 532 nm diode pump solid state (DPSS) laser. The shunts are caused by residual boron (p^+) diffusion within the phosphorus (n^+) diffused region following the trench etch that separates the p and n regions. Photoluminescence (PL) imaging showed that apparent shunt regions were removed following this process. Analysis of ABC solar cells by dark IV characterisation further confirmed that the shunt resistance was increased by about 30-fold (350 to 11500 $\Omega.cm^2$). The effective removal of shunts has increased the cell efficiency by 0.5% absolute. Carrier recombination induced by laser damage appears to be minimal since open-circuit voltage of the ABC cells barely changes for pre- and post-laser ablation, although more detailed investigations are required.

Keywords: Back Contact, Shunts, Dark I-V, Laser Processing, Photoluminescence.

1. INTRODUCTION

An all-back-contact (ABC) solar cell design, in conjunction with n-type silicon substrate, provides a number of advantages over standard front contacted cells. Interdigitated rear contacts offer benefits such as zero shading loss from metal fingers at the front surface, reduced grid resistance, improved front surface passivation and blue response since the competing requirement of lateral current transport in the front emitter is removed, high rear internal reflectance owing to the presence of a thick dielectric and near full metal coverage [1-3]. Furthermore, ABC cells have the advantage of simpler cell interconnection and superior aesthetic appearance. Utilisation of n-type material leads to reduced light-induced degradation due to the absence of the boron-oxygen complex and improved resilience to metallic impurities [4].

As part of a collaboration between PV manufacturer Trina Solar and the Solar Energy Research Institute of Singapore (SERIS), ANU is developing laboratory-scale ABC silicon solar cells on n-type wafer substrates (FZ and Cz) [5]. Since the development work at ANU commenced in April 2011, encouraging cell efficiencies have been achieved [6, 7]. In this paper, we describe further progress in ABC cell development at ANU. In particular, we demonstrate the technique of identifying and removing metallisation-induced shunt defects via laser isolation, and discuss the characterisation of shunts by PL imaging and dark IV analysis.

2. CELL DESIGN AND FABRICATION

The design of the ABC silicon solar cells reported in this paper is shown in Figure 1. The cell is fabricated on n-type <100> FZ wafers, thinned down to a final thickness of 200 µm. The cells are random pyramid textured at the sunward side, and have a passivation / ARC stack of thin thermally grown oxide (~20 nm) and PECVD silicon nitride (~50 nm) at both front and the chemically polished rear. The rear oxide / nitride stack provides rear surface passivation and also provides isolation of the metal grid from the underlying silicon. The cell incorporates a phosphorus front surface field (FSF) and alternating boron and phosphorus diffusions below p+ and n+ contacts respectively. The alternating n and p regions are fabricated on a pitch of 650 µm, with approximately 25% and 75% coverage respectively. Vacuum evaporated Aluminium, as thick as 3 µm, makes contact to the diffusions via point contacts through the rear oxide and nitride stack.

Fabrication begins with saw-damage etching the 1 Ω.cm 300 µm thick n-type FZ wafers. Wafers are then subjected to a phosphorus tube diffusion (40 Ω/□ at end of process) with in-situ oxide growth on both front and rear surfaces. Next, a thin LPCVD nitride is deposited on the entire wafer. Reactive Ion Etching (RIE) is used to remove the front LPCVD nitride, followed by removal of the underlying oxide in 10% HF. The front surface diffusion is etched off in TMAH followed by random pyramid texturing and removal of masking layers. The light phosphorus FSF (190 Ω/□) is then formed, and a masking oxide is grown via steam oxidation before lithographically defining the rear p^+ regions of the cell. A subsequent TMAH etch of approximately 2 µm depth removes the phosphorus doping from these defined regions in preparation for junction formation via a boron tube diffusion (80 Ω/□).

The masking oxide is removed, followed by thin oxide growth, forming gas anneal, and PECVD silicon nitride deposition on both front and rear. A pattern of small contact openings are created on the rear by non-aligned lithographic means, followed by vacuum-evaporation of aluminium of thickness up to ~3 µm. Finally, interdigitated metal fingers are realised by lithography-assisted aluminium etch. The samples are then annealed in forming-gas, followed by dicing the cells out of the wafer for IV measurement.

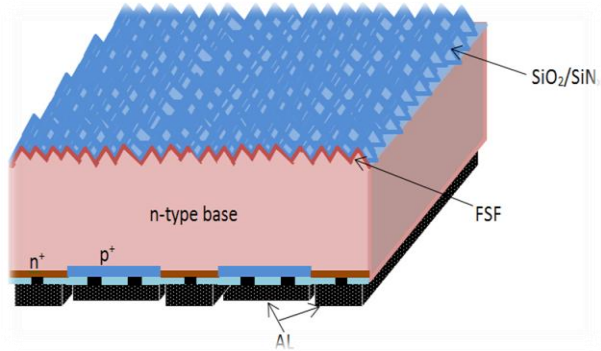

Figure 1: ABC Silicon Solar Cell Design.

3. SHUNT-LIMITED CELL PERFORMANCE

Several batches of cells have been fabricated according to the process description above. However, the cells reported in this study constitute a single batch of three completed cells, each of which exhibit efficiencies significantly limited by identifiable and rectifiable shunts. Of these cells, one only was initially diced out of its host wafer and measured for light I-V performance using the aperture areas of 13 cm^2 (3.6 x 3.6 cm) and 16 cm^2 (4 x 4 cm). Table 1 shows the I-V characteristics of the cell under one-sun illumination using a constant light source solar simulator. The cell efficiency is 21.6% and 20.8% for aperture-areas of 13 cm^2 and 16 cm^2 respectively. However, the illuminated I-V curve and also subsequently measured dark I-V curve clearly identifies a low shunt resistance which limits the cell efficiency. An ohmic shunt resistance of 350 $\Omega.cm^2$ is determined by fitting to the dark I-V curve.

Figure 2 shows the dark I-V curves of all three cells, with shunt resistance (R_{sh}) and dark series resistance ($R_{s\text{-}dark}$), as determined by curve-fitting, shown for each cell. R_{sh} is low in each case but not consistent between cells, indicative of sporadic rather than repeatable shunts (as would result from a mask defect). Meanwhile $R_{s\text{-}dark}$ suggests that series resistance is also limiting illuminated cell efficiency significantly, but the value is consistent between cells. The efficiency of the measured cell is reduced by ~0.5% by the presence of the shunt, as deduced from the conventional circuit model of a solar cell.

Table 1: Performance of an ABC cell under one-sun illumination for the aperture area of 13 cm^2.

	V_{oc} (mV)	J_{sc} (mA/cm^2)	FF	Eff (%)
14.1A	679	40.7	0.78	21.6

4. TECHNIQUE OF SHUNTS REMOVAL

Shunts have been observed in many types of solar cells and for many reasons, including laser scribing damage[8-11], tunnelling effects[12] due to juxtaposition of opposing diffusion regions (n^+ and p+), in devices passivated with a floating junction at the rear of the cell [13, 14], and in devices with an inversion layer induced by a dielectric layer (e.g. SiN_x), with high fixed positive charges, connecting the front metal grid (e.g. n+) and rear metal (e.g. p+) [8, 15, 16]. Laser Isolation shunt recoveries have been researched and demonstrated by many authors [17, 18]. However, laser isolation causes crystal damages in the cells leading to high carrier recombination affecting the cell conversion efficiency [19, 20] – particularly if left unpassivated as it is the end of the fabrication process. Here, we describe the removal of shunt by laser-assisted means to increase the cell efficiency.

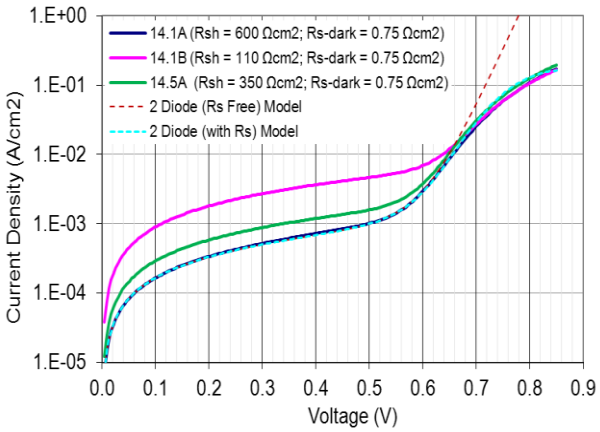

Figure 2: I-V curves of cells under dark illumination conditions. Dotted lines represent the 2-diode model fits to extract R_{sh} and $R_{s\text{-}dark}$.

Prior to the removal of shunts, the cause of shunts was investigated by visual inspection of the finished cells. The investigation revealed that evaporated aluminium was joining both n- and p-fingers due to residual p^+ diffusion in n^+ diffusion regions (Figure 3a). This incursion of the p^+ diffusion into the n^+ diffused regions is due to a lithography defect, likely due to particle contamination. Similar shunted regions were also observed in other cells (14.1A and 14.5A).

Shunts exist whenever the n finger metal makes contact to the underlying p^+ diffusion via dot contact openings (~ 5 µm diameter) in the dielectric. Removing the metal from these dots and thus isolating the diffused layer from the neighbouring metallised regions can be used to successfully remove the shunts. The shunt removal process, described with the aid of figure 3, begins by spin-coating photoresist (AZ1518), which is used as a protective layer for subsequent laser treatment, on the rear of the ABC cell (Figure 3a) followed by hard-baking. A diode pumped solid state (DPSS) Nd:YVO_4 laser operating at 532 nm is then used at low fluence (approximately 2 J/cm^2) to remove the photoresist from above the contact dots by forming approximately 50 µm diameter shapes which encircle the shunted dots (Figure 3b). The laser removal of photoresist, a combination of melting and ablation, exposes the metal that makes

contact to both p- and n-diffusions. Following the laser process, buffered HF is used to remove any oxide grown on top of aluminium, followed by etching of aluminium in an etch solution (20:4:1 - H_3PO_4:H_2O:HNO_3) at a temperature of 50 ^oC for 5 min to selectively remove the exposed aluminium (Figure 3c). After the aluminium etch, the protective photoresist layer was removed completely in acetone.

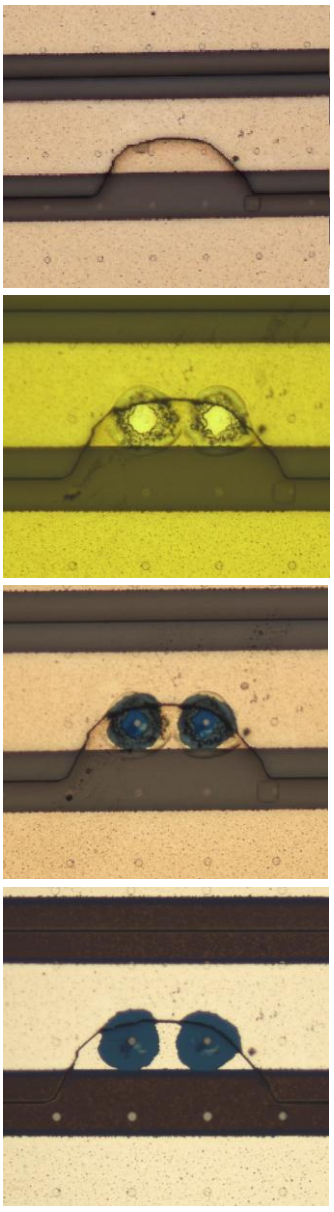

Figure 3: The technique of removing the shunts in ABC cells. The incursion with contact openings is identified (a), 532nm DPSS laser is used to remove resist (b), Aluminium is etched back (c) and resist removed (d).

5. RESULTS AND DISCUSSION

Following the removal of shunts, dark IV measurement was performed on the cells to analyse the behaviour of shunt resistance. As shown in the dark I-V curve of Figure 4, the ABC cell (14.5A) after shunt removal has a 30-fold increase in shunt resistance. The photoluminescence (PL) imaging technique was also used to identify the shunt appearances on the cells. PL imaging technique has been widely used in detecting shunts and shunt-induced damages [21-24]. Figure 5a shows an uncalibrated PL image of the shunted cell prior to the laser-assisted shunt removal. We can see two dark lines with very low PL counts where the apparent shunting (Figure 3a) occurs. Kasemann*et. Al* discussed that when using PL to detect shunts, the shunts will result in low PL intensities since a low junction voltage is maintained in the vicinity of the shunt and the shunts drain carriers from the surrounding regions of the cell [21]. Following shunt removal, it is noticeable from the PL image of Figure 5b that two apparent dark shunted lines have disappeared, with an increase in PL intensity in these regions.

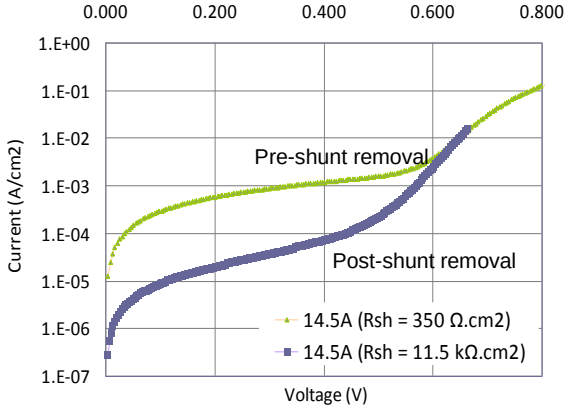

Figure 4: Dark IV measurement of the shunted cell before and after the shunt removal.

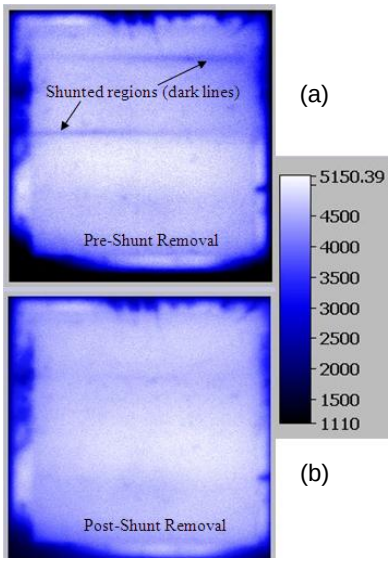

Figure 5: PL scan images of ABC cell before and after the shunt removal.

Following the shunt removal, the I-V performance of the cells was re-measured under one-sun illumination intensity, as plotted in figure 6. Electrical parameters of ABC cells after shunt-removal is shown in table 2. The cell which previously measured 21.6% under the 13 cm^2 aperture that excluded the busbars, prior to shunt removal, has now recorded an efficiency of 22.1%. The shunt removal process has increased the efficiency by

about 0.5%, the increase coming from the improvement in fill factor (*FF*), with no significant change in open-circuit voltage (V_{oc}) and current-density (J_{sc}) being observed. The increase in cell efficiency after shunt removal is in close agreement with the predicted cell performance for a shunt resistance greater than 2000 Ω.cm^2.

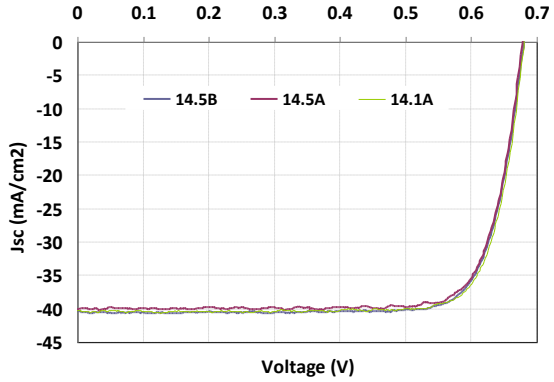

Figure 6: Performance of the ABC cell under one-sun illumination following the shunt removal for the aperture area testing of 13 cm^2.

Table 2: One-sun electrical parameters of ABC cells (13-cm^2) following the shunt removal. [1]Pre-laser assisted shunt removal. [2]Post-laser assisted shunt removal.

	Voc (V)	Jsc (mA/cm2)	FF	Efficiency (%)
14.1A[1]	0.679	-40.7	0.78	21.6
14.1A[2]	0.680	-40.3	0.81	22.1
14.5A	0.678	-40.0	0.81	21.7
14.5B	0.680	-40.5	0.80	22.1

Further optimisations of ABC cells in areas of improving the FSF, which results in reduction in front surface J_{oe} by 22 fA/cm^2; optimising the thickness of anti-reflection coating (ARC), leading to reduction in average reflectance across the range of 300-1200 nm by 4%; incorporation of aligned metal contact dots and optimised phosphorus diffusion, reducing the total series resistance (illuminated) by 0.08 Ωcm^2 have further increased the ABC cell efficiency to 22.6% for 13-cm^2 (excludes busbars) and 21.7% for 16-cm^2 (includes busbars).

Table 3: One-sun electrical parameters of ABC cells (13-cm^2) following further optimisations.

	Voc (V)	Jsc (mA/cm2)	FF	Efficiency (%)
15.6A	0.679	-40.6	0.81	22.5
15.6B	0.681	-40.9	0.81	22.6

6. CONCLUSIONS

Since the project commenced in April 2011, the development of high-efficiency ABC cells on n-type substrate (FZ or Cz) at ANU, as part of the collaboration between the Trina Solar and SERIS is ongoing. Although the development work is just a little less than a year, the progress made at ANU is indeed encouraging. Shunt removal assisted by 532 nm diode pumped solid state laser was realised on the ABC cells, with shunt resistance measured from dark I-V curves increasing from for example 350 Ω.cm^2 to around 11.5 kΩ.cm^2 in the case of one cell. Shunt detection via PL imaging also confirms that localised shunts are indeed removed by the laser treatment. After the shunt removal, cells show an approximate 30-fold increase in R_{sh} and an efficiency gain of 0.5% was observed for one cell. As a result, the aperture-area (13 cm^2) efficiency of the best cell produced increased, after shunt removal, to 22.1%. Further optimisations in areas of FSF, ARC and contact resistance have led the efficiency gain of best ABC cell by another 0.5% absolute.

ACKNOWLEDGEMENTS

Funding of this work by Trina Solar is acknowledged. The Solar Energy Research Institute of Singapore (SERIS) is sponsored by the National University of Singapore and Singapore's National Research Foundation through the Singapore Economic Development Board.

REFERENCES

[1] R. M. Swanson, A.K. Beckwith, R.A. Crane, W.D. Eades, Y.H. Kwark, R.A. Sinton, "Point-contact silicon solar cells," *IEEE Transactions on Electron Devices,* vol. 31, pp. 661–664, 1984.

[2] R. A. Sinton and R. M. Swanson, "Simplified backside-contact solar cells," *Electron Devices, IEEE Transactions on,* vol. 37, pp. 348-352, 1990.

[3] R. A. Sinton, "Bilevel contact solar cells," ed: Google Patents, 1991.

[4] D. Macdonald and L. J. Geerligs, "Recombination activity of interstitial iron and other transition metal point defects in p- and n-type crystalline silicon," *Applied Physics Letters,* vol. 85, pp. 4061-4063, 2004.

[5] *Trina Solar Limited, Press release, Trina Solar and SERIS to develop high efficiency solar cells, http://phx.corporate-ir.net/phoenix.zhtml?c=206405&p=irol-newsArticle&ID=1432729&highlight=, June 2010.*

[6] N. Zin, A. Blakers, K. McIntosh, E. Franklin, T. Kho, J. Wong, T. Mueller, A. G. Aberle, Z. Feng, Q. Huang, "19% Efficient N-Type All-Back-Contact Silicon Wafer Solar Cells With Planar Front Surface," presented at the the Australian and New Zealand Solar Energy Society Sydney, Australia, 2011.

[7] N. Zin, A. Blakers, E. Franklin, T. Kho, K. McIntosh, J. Wong, T. Mueller, A. Aberle, Y. Yang, X. Zhang, Z. Feng, and Q. Huang, "Progress in the development of All-Back-Contacted Silicon Solar Cells," presented at the PV Asia Pacific Conference 2011, Singapore, 2011.

[8] O. Breitenstein, *et al.*, "Shunt types in crystalline silicon solar cells," *Progress in Photovoltaics: Research and Applications,* vol. 12, pp. 529-538, 2004.

[9] O. Breitenstein, *et al.*, "Shunts due to laser scribing of solar cells evaluated by highly sensitive lock-in thermography," *Solar Energy Materials and Solar Cells,* vol. 65, pp. 55-62, 2001.

[10] F. Granek, *et al.*, "A Systematic Approach to Reduce Process-Induced Shunts in Back-Contacted MC-Si Solar Cells," in *Photovoltaic Energy Conversion, Conference Record of the 2006 IEEE 4th World Conference on*, 2006, pp. 1319-1322.

[11] O. Breitenstein, J. Rakotoniaina, M. Al Rifai, M. Werner, "Shunt types in crystalline silicon solar cells," *Progress in Photovoltaics: Research and Applications,* vol. 12, pp. 529-538, 2004.

[12] J.-H. Guo, *et al.*, "Investigations of parasitic shunt resistance in n-type buried contact solar cells," *Progress in Photovoltaics: Research and Applications,* vol. 14, pp. 95-105, 2006.

[13] C. B. Honsberg, *et al.*, "Elimination of parasitic effects in floating junction rear surface passivation for solar cells," in *Photovoltaic Specialists Conference, 1996., Conference Record of the Twenty Fifth IEEE*, 1996, pp. 401-404.

[14] O. Breitenstein, *et al.*, "Localization of shunts across the floating junction of DSBC solar cells by lock-in thermography," in *Photovoltaic Specialists Conference, 2000. Conference Record of the Twenty-Eighth IEEE*, 2000, pp. 124-127.

[15] S. Dauwe, *et al.*, "Experimental evidence of parasitic shunting in silicon nitride rear surface passivated solar cells," *Progress in Photovoltaics: Research and Applications,* vol. 10, pp. 271-278, 2002.

[16] I. Cesar*, et al.*, "All-side SiNx passivated mc-Si solar cells evaluated with respect to parasitic shunting," in *Photovoltaic Specialists Conference (PVSC), 2009 34th IEEE*, 2009, pp. 001386-001391.
[17] T. T. M. D. Abbott, H. P. Hartmann, R. Gupta, and O. Breitenstein, "Laser isolation of shunted regions in industrial solar cells," *Progress in Photovoltaics: Research and Applications,* vol. 15, pp. 613-620, 2007.
[18] T. P. J. Arumughan, A. Hauser, and I. Melnyk, "Simplified edge isolation of buried contact solar cells," *Solar Energy Materials and Solar Cells,* vol. 87, pp. 705-714, 2005.
[19] M. Abbott, P. Cousins, F. Chen, J. Cotter, "Laser-induced defects in crystalline silicon solar cells," in *Photovoltaic Specialists Conference, 2005. Conference Record of the Thirty-first IEEE*, 2005, pp. 1241-1244.
[20] N. Zin and A. Blakers, "Performance of Miniature Silicon Solar Cells," in *Procceeding of 24th EUPVSEC*, Valencia, Spain, 2010.
[21] M. Kasemann, D. Grote, B. Walter, W. Kwapil, T. Trupke, Y. Augarten, R. A. Bardos, E. Pink, M. D. Abbott, W. Warta, "Luminescence imaging for the detection of shunts on silicon solar cells," *Progress in Photovoltaics: Research and Applications,* vol. 16, pp. 297-305, 2008.
[22] O. Breitenstein, J. Bauer, T. Trupke, R. A. Bardos, "On the detection of shunts in silicon solar cells by photo- and electroluminescence imaging," *Progress in Photovoltaics: Research and Applications,* vol. 16, pp. 325-330, 2008.
[23] M. Kasemann, M. C. Schubert, T. Manuel, M. Kober, M. Hermle, W. Warta., "Comparison of luminescence imaging and illuminated lock-in thermography on silicon solar cells," *Applied Physics Letters,* vol. 89, p. 224102, 2006.
[24] T. Trupke, R. A. Bardos, M. D. Abbott, F. W. Chen, J. E. Cotter, A. Lorenz, "Fast Photoluminescence Imaging of Silicon Wafers," in *Photovoltaic Energy Conversion, Conference Record of the 2006 IEEE 4th World Conference on*, 2006, pp. 928-931.